Selective Production of Carbon Monoxide via Methane Oxychlorination over Vanadyl Pyrophosphate

Selective Production of Carbon Monoxide *via* Methane Oxychlorination over Vanadyl Pyrophosphate

Vladimir Paunović, Guido Zichittella, Réne Verel, Amol P. Amrute, and Javier Pérez-Ramírez*

Abstract: A catalytic process is demonstrated for the selective conversion of methane into carbon monoxide *via* oxychlorination chemistry. Therein, HCl is added to a CH_4-O_2 feed to facilitate the C-H bond activation under mild conditions, leading to the formation of chloromethanes, CH_3Cl and CH_2Cl_2. The latter are oxidized *in situ* over the same catalyst, yielding CO and recycling HCl. A material exhibiting chlorine evolution *via* HCl oxidation, high activity to oxidize the chloromethanes into CO, and no ability to oxidize CO is therefore essential to accomplish this target. Following these design criteria, vanadyl pyrophosphate (VPO) was identified as an outstanding catalyst, exhibiting a CO yield up to ~35% at 96% selectivity and a stable behavior. These findings constitute a basis for the development of a process enabling the on-site valorization of the stranded natural-gas reserves using CO as a highly versatile platform molecule.

Methane, the principal constituent of natural gas, is an important energy resource and an attractive feedstock for the manufacture of chemicals and fuels.[1] However, >30% of the abundant natural-gas reserves are allocated in small reservoirs and/or remote areas, wherein the high transportation costs of methane and marked capital expenditure of the existing syngas-based gas-to-liquid (GTL) technologies hamper their efficient exploitation.[1a,b,2] Consequently, copious amounts of natural gas retrieved from these stranded wells are nowadays burnt to reduce the anthropogenic greenhouse gas emissions - the global warming potential of CH_4 is ≥21 times higher than that of CO_2. Disparagingly, the so-called flaring wastes around 3.5% of the global natural gas production - a quantity worth *ca.* 13 billion USD and comparable to the current fraction of the world's natural gas supply which is used for the manufacture of commodities (<10%).[1d,3] This alarming situation calls for the development of modular, decentralized processes for the economical harvesting of the stranded gas.[1b,2a]

The catalytic oxyhalogenation of methane, comprising its reaction with a hydrogen halide (HCl or HBr) and oxygen, is an attractive approach to satisfy these objectives as it enables direct methane functionalization under moderate operating conditions (≈~1 bar, <853 K).[4-6] This route has traditionally targeted the production of methyl halides (CH_3Cl and CH_3Br), platform molecules equivalent to methanol that can be transformed into a wide spectrum of value-added chemicals and fuels *via* the halogen elimination step in the form of hydrogen halide. Recent reports demonstrated the high selectivity to halomethanes over LaOCl and CeO_2 in oxychlorination, and over CeO_2 and vanadyl pyrophosphate (VPO) in oxybromination.[4-6] Moreover, the oxyhalogenation of methane over catalysts with mild oxidizing properties such as LaOCl in oxychlorination, and $FePO_4$ and VPO in oxybromination led to CO as the dominant oxidation product, with only marginal CO_2 production.[4a,5-7]. These findings hint an extra potential of the route in the form of an effective method to exploit the natural gas feedstock for on-purpose CO production, which is a key building block in the manufacture of numerous commodities.[8] In this way, the highly endergonic steam- reforming and coal gasification, commonly practiced today to obtain CO, could be substituted by an exergonic halogen-mediated process. Nevertheless, this application of the oxyhalogenation reaction has not been considered to date, probably due to the fact that CO was never produced at a selectivity exceeding 50%,[4,6,7] which would necessitate complex downstream separation train. Alternatively, a two-step process can be sought, involving the selective methane oxyhalogenation over one catalyst, followed by the oxidation/hydrolysis into CO over a second catalyst.[9] Although the latter step was typically studied with an aim to convert the halomethanes into CO_2, catalysts such as alumina and La-based materials could yield CO with a relatively high selectivity, which however depends on the nature of a halomethane.[9c] Still, an integration of the ha,lomethane formation with their oxidation/dehydrochlorination into CO over a single catalyst is highly desirable in view of process intensification, but is rather challenging from the point of catalyst design as it requires a fine balance between the catalyst activities in two reactions. In such a hypothetical process, the use of HCl as a halogenating agent would be desirable instead of HBr due to the lower corrosiveness and the much higher availability of the former.[10]

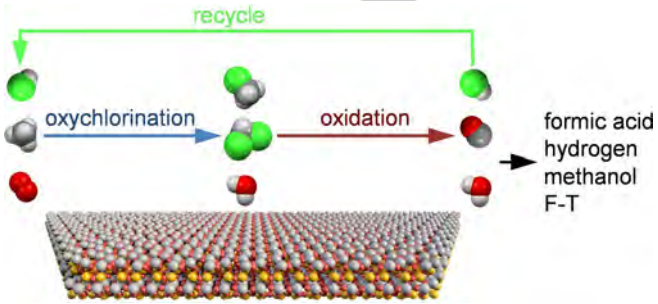

Figure 1. CO is the chief carbonylating agent for the production of a wide variety of commodities such as acids, alcohols, and isocyanates. The integration of the oxychlorination of methane with the selective oxidation of the thus obtained chloromethanes into CO over a single catalytic material is an attractive route to valorize stranded natural gas basins.

[*] V. Paunović,[+] G. Zichittella,[+] Dr. A. P. Amrute, Dr. R. Verel, Prof. J. Pérez-Ramírez
Institute for Chemical and Bioengineering
Department of Chemistry and Applied Biosciences, ETH Zurich
Vladimir-Prelog-Weg 1, 8093 Zurich, Switzerland
E-mail: jpr@chem.ethz.ch

[+] Equal contribution

Supporting information for this article is given *via* a link at the end of the document.

Herein, we present the one-step selective conversion of CH_4 into CO *via* oxychlorination chemistry (Figure 1) as an alternative route to valorize the emerging natural-gas feedstock given the great versatility of CO,[7-8] *in situ* HCl recycling, as well as the reaction exothermicity, enabling heat integration in the subsequent CO-processing steps. Thereby, it is essential to find a catalyst showing a high activity for the oxychlorination of methane to chloromethanes and strong propensity for the selective oxidation of the latter into CO under oxychlorination conditions (Figure 1).

To approach the above targeted catalytic process, a series of bulk materials comprising RuO_2, CeO_2, $LaVO_4$, Nb_2O_5, TiO_2, and VPO having different oxidation properties,[6,11] were prepared and characterized by X-ray diffraction and N_2 sorption, respectively (Figure S1, Table S2). Their performance in the oxychlorination of methane is compared by taking the temperature at which *ca.* 15% CH_4 conversion is achieved, T_{15}, as a relative measure of their overall catalytic activity (Figure 2, top), while product distribution at this relatively low conversion level was used to fingerprint their inherent reaction kinetics (Figure 2, bottom). The results are presented on the basis of an increasing selectivity to CO, which is considered here as the principal descriptor of the catalyst performance. Based on their activity patterns, the catalysts can be classified into four different categories. The first class is represented by RuO_2, a well-established HCl oxidation catalyst,[10a] exhibiting the highest activity for methane conversion as inferred from its lowest value of T_{15}. Nevertheless, the oxychlorination reaction over this material leads to a pronounced CO_2 formation, as can be expected from its strong propensity to oxidize CH_4, chloromethanes, and possible CO intermediate into CO_2.[6,12] On the other hand, CeO_2 predominantly produces chloromethanes, in line with previous studies reporting its outstanding selectivity to these products in the oxyhalogenation reaction.[5,6] The third class of catalysts comprises mild oxidizers such as $LaVO_4$ and Nb_2O_5,[11] exhibiting low activity for CH_4 conversion (the highest values of T_{15}) (Figure 2). Although CO is the dominant oxidation product, a significant part of the chloromethanes remains unconverted even at high reaction temperatures, hampering thus the closure of the HCl loop. Finally, TiO_2 and VPO show inherently high selectivity to CO and moderate activity in converting CH_4. The unprecedentedly suppressed CO_2 formation over VPO (≤1% in selectivity) coupled to the low residual amounts of chloromethanes, make it a highly attractive catalyst for the selective CO production from methane *via* oxychlorination chemistry. This unique performance of VPO and TiO_2 is understood *via* a series of catalytic tests (Figure S2, Figure 3). In contrast to CeO_2 and RuO_2, where evolution of CO_2 is enhanced at high reaction temperatures (Figure S2), in the oxychlorination of methane over TiO_2 and particularly VPO, the production of CO_2 remains low in a very broad temperature range (Figures 3a,b). In case of VPO, 33% yield and 96% selectivity for CO are achieved at 836 K. Only trace amounts of H_2 are detected, while HCl conversion is ≤1.5% (Table S3), which suggests that the biggest part of HCl is recycled *in situ* in a single reactor pass. The selectivity to CO and CO_2 generally increases and that to halomethanes decreases (Figure S2, Figures 3a,b) upon raising the reaction temperature, suggesting the consecutive oxidation of the chloromethanes generated in the first oxychlorination step as the plausible pathway of carbon oxide formation. Nevertheless, the latter products might in principle evolve from the direct oxidation of methane over a

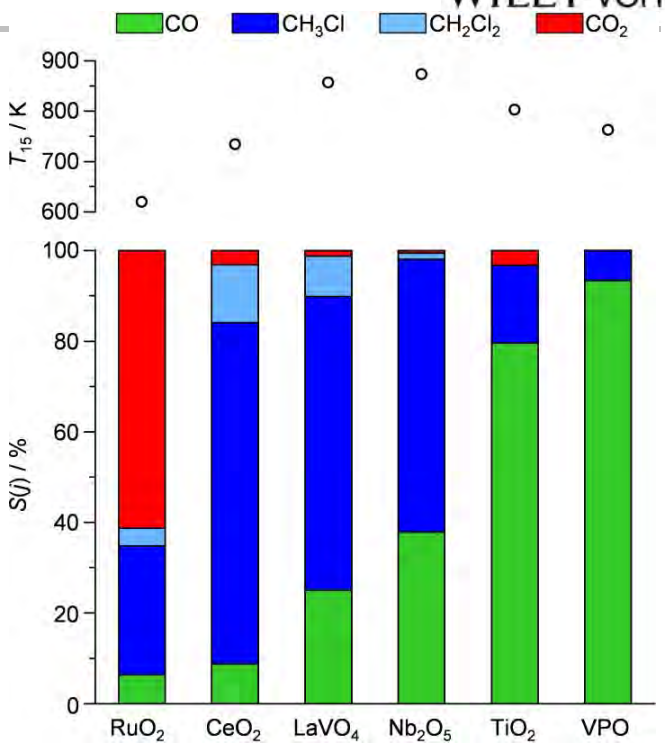

Figure 2. Selectivity to product *j*, *S*(*j*), in the oxychlorination of methane over various catalysts at *ca.* 15% of CH_4 conversion, which is obtained at temperature T_{15} indicated in the top plot. Full set of experiments is presented in Figure S2. Conditions: F_T/W_{cat} = 100 cm^3 min^{-1} g^{-1}, feed molar composition CH_4:HCl:O_2:Ar:He = 6:6:3:4.5:80.5, and P = 1 bar.

catalyst. To elucidate the contribution of these two routes to the CO formation over VPO and TiO_2, the direct oxidation of methane (Figure 3a, open symbols) as well as the impact of feed HCl concentration on reaction performance (Figure S3) were also studied. The negligible CH_4 conversion over both VPO and TiO_2 in the direct oxidation at temperatures which are significantly higher compared to those applied in the oxychlorination reaction and an increase in CH_4 conversion upon increasing the inlet HCl concentration, demonstrates the pivotal role of HCl in activating methane and corroborates the oxidation of halomethanes as the principal source of CO over these two catalysts. To support the above-indicated consecutive pathway, the activities of VPO and TiO_2 in the oxidation of chloromethanes are further assessed as presented in Figures 3c-f. In good agreement with the oxychlorination tests, CO is produced with very high selectivity (>99%) in both CH_3Cl and CH_2Cl_2 oxidation over VPO (Figures 3d,f), while in case of TiO_2, the selectivity to CO observed in the oxidation of CH_3Cl (≈90%) is lower than that obtained in the oxidation of CH_2Cl_2 (>99%). Besides, the light-off curves for the conversion of chloromethanes over TiO_2 are shifted to lower temperatures than that over VPO, indicating its higher activity in these reactions, which at first glance contrasts the results presented in Figures 2 and 3b. This might be explained by the substantially higher activity of VPO in the HCl oxidation reaction (Figure 3h), indicating the higher propensity of this catalyst to evolve chlorine, and thus the enhanced production of the precursor chloromethanes, leading to a higher CO productivity. Besides, inhibition of the chloromethanes oxidation by HCl poisoning of TiO_2, which has been often reported in the catalytic abatement of chlorocarbons over oxide materials, might also contribute to the difference in performance among the two catalysts.[9c,13] To check for the latter effect, HCl was co-fed with CH_2Cl_2 and O_2 in the corresponding oxidation test to simulate the conditions of the oxychlorination reaction (Figures 3e,f). The results demonstrate

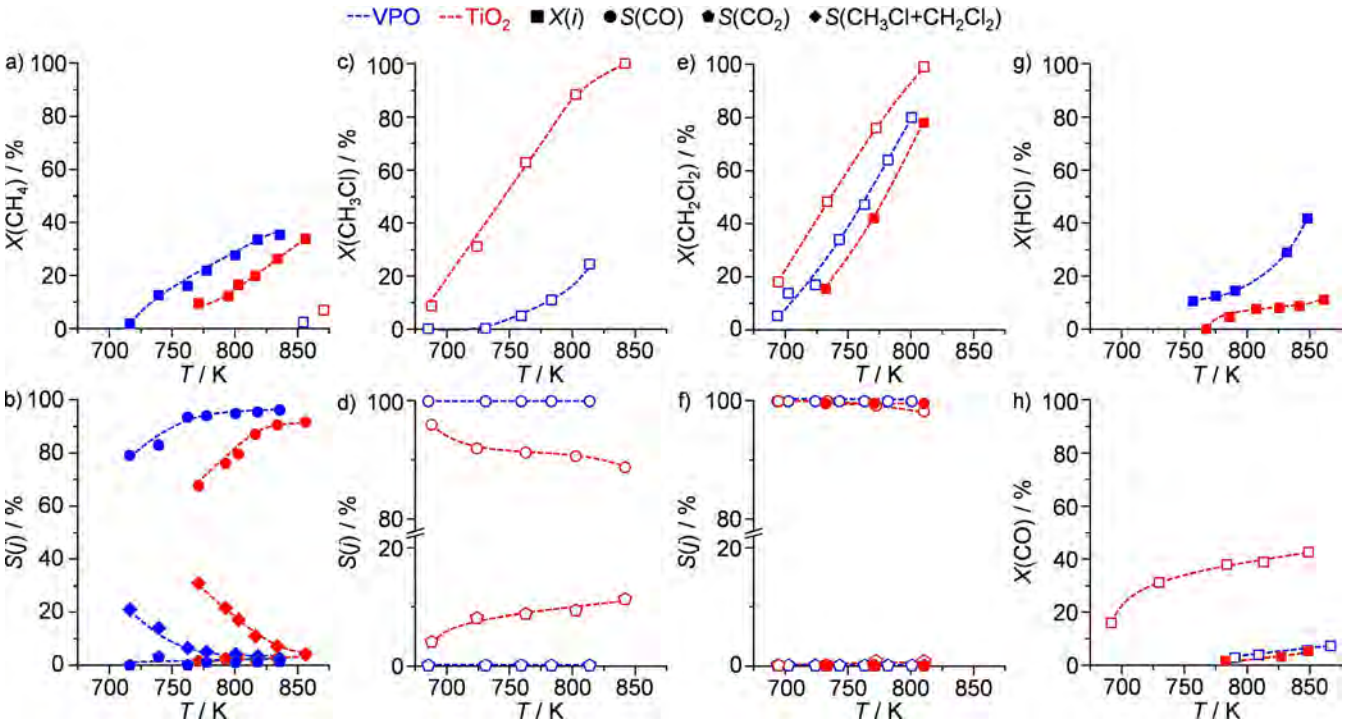

Figure 3. Conversion of reactant *i*, *X*(*i*), and selectivity to product *j*, *S*(*j*), over VPO (blue) and TiO_2 (red) *versus* temperature in: a, b) methane oxychlorination (CH_4:HCl:O_2:Ar:He = 6:6:3:4.5:80.5) and oxidation (CH_4:O_2:Ar:He = 6:3:4.5:86.5); c, d) CH_3Cl oxidation (CH_3Cl:O_2:Ar:He = 1:3:4.5:91.5); e, f) CH_2Cl_2 oxidation (CH_2Cl_2:O_2:HCl:Ar:He = 1:3:0(6):4.5:91.5(85.5)); g) HCl oxidation (HCl:O_2:He = 6:3:91); and h) CO oxidation (CO:O_2:HCl:Ar:He = 1:3:0(6):4.5:91.5(86.5)). Open symbols denote the points taken in the absence of HCl in the feed. Conditions: F_T/W_{cat} = 100 cm^3 min^{-1} g^{-1} and P = 1 bar.

a significant drop in CH_2Cl_2 conversion over TiO_2 in the presence of HCl, thus corroborating the inhibitory role of HCl, contributing to the inferior activity of this material compared to VPO in the oxychlorination of methane.

The differences in performance of VPO and TiO_2 in the oxychlorination reaction, as well as those in the oxidation of halomethanes, are further explained by evaluating their activities in CO oxidation (Figure 3h, open symbols). VPO shows much lower conversion of CO into CO_2 than TiO_2 (Figure 3h), which is likely caused by its inherently low propensity to adsorb CO.[14] Nevertheless, in analogy to the CH_2Cl_2 oxidation, CO conversion over TiO_2 is substantially suppressed in the presence of HCl (Figure 3h, closed symbols), which might explain the low CO_2 productivity observed in the oxychlorination of methane.

Based on these results, the CO production from CH_4 over VPO can be rationalized by the mechanism comprising HCl oxidation into Cl_2, followed by the gas-phase methane chlorination, which is analogue to that proposed for the methane oxybromination over this material.[6] This is supported by the ability of VPO to oxidize HCl into Cl_2 (Figure 3g), and its low activity in the direct oxidation of methane (Figure 3a), indicating its minor propensity to cleave C-H bonds. Moreover, the temperature window of the HCl oxidation coincides with that of methane oxychlorination, suggesting that the evolved Cl_2 readily reacts with methane. This is in line with literature reports testifying the vigorous kinetics of methane chlorination already at 673 K,[1c] and it is also corroborated by the low Cl_2 concentration detected at the reactor outlet (Table S3). The ability of VPO to oxidize HCl at temperatures that are comparable or even higher than those needed for chloromethanes oxidation is uniquely combined with its inherent propensity to suppress the oxidation of CO into CO_2, eventually resulting in a highly selective production of CO from methane *via* the oxychlorination reaction. It is interesting to note that the oxybromination reaction over VPO yields CO as the principal oxidation product. Still, the generation of CO is generally overwhelmed by the formation of bromomethanes, even at high reaction temperatures,[6] which might be explained by the significantly faster HBr oxidation compared to bromomethanes oxidation (Figure S4). The exceptional CO production via methane oxychlorination over VPO is shown to be stable by a 100 h on stream test (Figure 4a). X-ray diffraction (XRD) analysis of the fresh and used samples recovered after different time-on-stream (Figure S5) indicated the equilibration of the starting $(VO)_2P_2O_7$ structure within the first 1 h of operation, which remains unaltered over the whole evaluated period of time. ^{31}P nuclear magnetic resonance by spin-echo mapping (Figure 4b) showed a major peak centered at around 2500 ppm, which is characteristic for $(VO)_2P_2O_7$ phase.[15] This peak is slightly broader in case of the fresh catalyst sample, but shows no significant changes among the used catalyst, in line with XRD

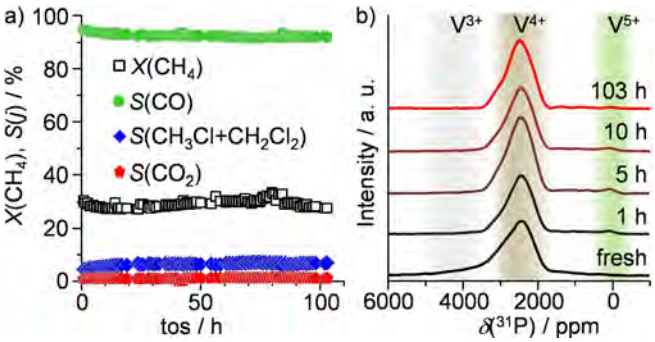

Figure 4. a) Methane conversion and product selectivity *versus* time-on-stream (tos) in the oxychlorination of methane over VPO. b) ^{31}P nuclear magnetic resonance spectra by spin-echo mapping of fresh and used VPO recovered after *x* h on stream. Conditions: F_T/W_{cat} = 100 cm^3 min^{-1} g^{-1}, CH_4:HCl:O_2:Ar:He = 6:6:3:4.5:80.5, T = 803 K, and P = 1 bar.

data. No peaks ascribed to V^{3+} phases (located at ca. 4700 ppm) could be observed, while a small peak allocated around 0 ppm, which is more pronounced in case of used catalyst samples indicates the presence of V^{5+} sites. This is further corroborated by temperature-programmed reduction with H_2 (Figure S5) and X-ray photoelectron spectroscopy (Table S4, Figure S6), which also pointed to the presence of V^{5+} sites in the surface region of all catalyst samples.

The unique performance of VPO opens a way for the development of a novel process for the natural gas upgrading by exploiting CO as a versatile platform molecule. In particular, if coupled with the well-established production of formic acid, a valued chemical and highly perspective energy carrier,[16] it could provide an effective means of bringing carbon, hydrogen, and/or energy equivalents of stranded methane reserves to the market in a liquid form. Alternatively, the on-site water-gas shift of the CO-H_2O mixture could generate hydrogen.[17] In this way, traditional syngas-to-chemicals transformations, such as methanol production or Fischer-Tropsch (FT) hydrocarbon synthesis, can be practiced by circumventing the steam-reforming (1073-1273 K, 20-30 bar) or auto-reforming (>2273 K, <100 bar) processes, which are the most energy- and capital-demanding steps of the commercial syngas generation technologies.[1,18] Moreover, H_2 derived from renewable sources, such as photocatalytic water splitting or biomass reforming,[19] might be also utilized.

In conclusion, we demonstrated for the first time the highly selective one-step CO production from methane *via* oxychlorination chemistry. Following the simple catalyst design criteria, stating that the optimal catalyst for this process should exhibit the chlorine evolution activity, essential to support the formation of chloromethanes, and the ability to selectively oxidize the latter into CO, various materials families comprising different redox properties were evaluated in the oxychlorination of methane. Herein, VPO, exhibiting a high selectivity to halomethanes in methane oxybromination, emerged as an outstanding catalyst for CO production *via* methane oxychlorination, demonstrating the complexity and versatility of the oxyhalogenation chemistry. A yield of CO up to ~35% at 96% selectivity was achieved over this catalyst under ambient pressure and temperatures <835 K. Its exceptional performance, which was stable over 100 h on stream, constitutes the basis for the development of a modular, decentralized process for the valorization of the stranded natural gas by exploiting CO as a well-established platform molecule for the manufacture of value-added commodities.

Experimental Section

Commercial CeO_2 was treated at 1173 K, while TiO_2-rutile and Nb_2O_5 were treated in static air at 873 K, respectively, prior to their use in the catalytic tests. RuO_2 was prepared by thermal decomposition of $RuCl_3$ at 823 K in static air. $LaVO_4$ was synthetized by co-precipitation of $La(NO_3)_3{\cdot}6H_2O$ with NH_4VO_4, followed by hydrothermal synthesis at 453 K for 24 h. After filtration and washing with water and methanol, the powder was dried in vacuum at 373 K and calcined at 873 K. VPO was prepared by refluxing a slurry containing V_2O_5, benzyl alcohol, and isobutyl alcohol for 3 h. Then, H_3PO_4 was added (P:V = 1.2) and the slurry was refluxed for 16 h, followed by drying in vacuum at 373 K and thermal treatment at 873 K under flowing nitrogen. A heating rate of 5 K min^{-1} and holding time of 5 h were applied in all thermal treatments of the catalysts. The catalytic tests were performed at 1 bar in a continuous-flow fixed-bed reactor set-up (Scheme S1) using a catalyst weight W_{cat} = 1.0 g (particle size = 0.4-0.6 mm) well-mixed with quartz (particle size = 0.2-0.3 mm) and a total gas flow F_T = 100 cm^3 STP min^{-1} at bed temperatures, T, in the range of 423-875 K. The molar composition of the mixtures in methane oxychlorination (CH_4:HCl:O_2:Ar:He = 6:6:3:4.5:80.5), methane oxidation (CH_4:O_2:Ar:He = 6:3:4.5:86.5), and the oxidation of CH_3Cl/CH_3Br (CH_3Cl/CH_3Br:O_2:Ar:He =1:3:4.5:91.5), CH_2Cl_2/CH_2Br_2 (CH_2Cl_2/CH_2Br_2:O_2:HCl/HBr:Ar:He =1:3:0(6):4.5:91.5(85.5)), HCl/HBr (HCl:O_2:Ar:He = 6:3:4.5:86.5), and CO (CO:O_2:HCl:Ar:He = 1:3:0(6):4.5:91.5(86.5)) were set using digital mass flow controllers to feed the gases, while CH_2Cl_2/CH_2Br_2 were fed by syringe pump and a home-made evaporation unit. Concentrations of the carbon-containing compounds at the reactor inlet and outlet were analyzed online using a gas chromatograph coupled to a mass spectrometer. The concentration of H_2 was determined by an off-line gas chromatograph equipped with a thermal conductivity detector. The Cl_2 concentration was quantified using an off-line iodometric titration of the absorbing KI solution, while the HCl concentration was determined by acid-base titration after its absorption into H_2SO_4 solution. The errors of carbon and chlorine balances were lower than 5%. The fresh and used catalysts were characterized by means of X-ray diffraction, N_2 sorption, X-ray fluorescence, temperature-programmed reduction with H_2, ^{31}P nuclear magnetic resonance spin-echo mapping, and X-ray photoelectron spectroscopy. More details on catalyst preparation, characterization, and testing are provided in the Supporting Information.

Acknowledgements

Funding by the Swiss National Science Foundation (project no. 200021-156107) and ETH Zurich (research grant ETH-04 16-1) is acknowledged. Nicolas Aellen is thanked for performing part of the catalytic tests. Dr. Roland Hauert is acknowledged for conducting X-ray photoemission spectroscopy measurements.

Keywords: C1 chemistry • carbon monoxide • heterogeneous catalysis • methane oxychlorination • natural-gas upgrading

[1] a) J. H. Lunsford, *Catal. Today* **2000**, *63*, 165-174; b) E. McFarland, *Science* **2012**, *338*, 340-342; c) G. A. Olah, A. Goeppert, G. K. Surya Prakash, *Beyond Oil and Gas: The Methanol Economy,* Wiley-VCH, Weinheim, **2009**, pp. 29-53 and pp. 249-251; d) R. Horn, R. Schlögl, *Catal. Lett.* **2015**, *145*, 23-39.

[2] a) J. A. Labinger, J. E. Bercaw, *Nature* **2002**, *417*, 507-514; b) R. Khalilpour, I. A. Karimi, *Energy* **2012**, *40*, 317-328; c) PetroWiki press release, 2016. Stranded gas, www.petrowiki.com, accessed June 5th, **2016**, 10:00 GMT.

[3] a) J. Tollefson, *Nature* **2016**, doi:10.1038/nature.2016.19141; b) U.S. Energy Information Administration, *Monthly Energy Review June 2016*, U.S. Department of Energy, Washington, U.S., **2016**.

[4] a) E. Peringer, S. G. Podkolzin, M. E. Jones, R. Olindo, J. A. Lercher, *Top. Catal.* **2006**, *38*, 211-220; b) S. G. Podkolzin, E. E. Stangland, M. E. Jones, E. Peringer, J. A. Lercher, *J. Am. Chem. Soc.* **2007**, *129*, 2569-2576.

[5] J. He, T. Xu, Z. Wang, Q. Zhang, W. Deng, Y. Wang, *Angew. Chem. Int. Ed.* **2012**, *51*, 2438-2442; *Angew. Chem.* **2012**, *124*, 2488-2492; b) Z. Guo, B. Liu, Q. Zhang, W. Deng, Y. Wang, Y. Yang, *Chem. Soc. Rev*. **2014**, *43*, 3480-3524.

[6] V. Paunović, G. Zichittella, M. Moser, A. P. Amrute, J. Pérez-Ramírez, *Nat. Chem.* **2016**, *8*, 803-809.

[7] R. Lin, Y. Ding, L. Gong, W. Dong, J. Wang, T. Zhang, *J. Catal.* **2010**, *272*, 65-73.

[8] J. Bierhals in *Ullmann's Encyclopedia of Industrial Chemistry, Vol. 6,* Wiley-VCH, Weinheim, **2012**, pp. 679-693.

[9] a) R. W. van den Brink, P. Mulder, R. Louw, G. Sinquin, C. Petit, J.-P. Hindermann, *J. Catal.* **1998**, *180*, 153-160; b) P. Van der Avert,

B. M. Weckhuysen, *Angew. Chem. Int. Ed.* **2002**, *41*, 4730-4732; *Angew. Chem.* **2002**, *114*, 4924-4926; c) P. Van der Avert, B. M. Weckhuysen, *Phys. Chem. Chem. Phys.* **2004**, *6*, 5256-5262. d) A. W. A. M. van der Heijden, M. Garcia Ramos, B. M. Weckhuysen, *Chem. Eur. J.* **2007**, *13*, 9561-9571; e) A. W. M. van der Heijden, S. G. Podkolzin, M. E. Jones, J. H. Bitter, B. M. Weckhuysen, *Angew. Chem. Int. Ed.* **2008**, *47*, 5002-5004; *Angew. Chem.* **2008**, *120*, 5080-5082; f) A. W. A. M. van der Heijden, A. J. M. Mens, R. Bogerd, B. M. Weckhuysen, *Catal. Lett.* **2008**, *122*, 238-246.

[10] a) J. Pérez-Ramírez, C. Mondelli, T. Schmidt, O. F.-K. Schlüter, A. Wolf, L. Mleczko, T. Dreier, *Energy Environ. Sci.* **2011**, *4*, 4786-4799; b) P. Schmittinger, T. Florkiewicz, L. C. Curlin, B. Lüke, R Scannel, T. Navin, E. Zelfel, R. Bartsch in *Ullmann's Encyclopedia of Industrial Chemistry*, *Vol. 8,* Wiley-VCH, Weinheim, **2012**, pp. 531-621; c) S. Boldyryev, P. S. Varbanov, *Chem. Eng. Trans.* **2014**, *39*, 1423-1428.

[11] a) C. T. Au, W. D. Zhang, H. L. Wan, *Catal. Lett.* **1996**, *37*, 241-246; b) M. Ziolek, *Catal. Today* **2003**, *78*, 47-64.

[12] H. Madhavaram, H. Idriss, S. Wendt, Y. D. Kim, M. Knapp, H. Over, J. Aßmann, E. Löffler, M. Muhler, *J. Catal.* **2001**, *202*, 296-307.

[13] Q. Dai, X. Wang, G. Lu, *Appl. Catal. B* **1999**, *81*, 192-202.

[14] G. Busca, G. Centi, F. Trifirò, V. Lorenzelli, *J. Phys. Chem.* **1986**, *90*, 1337-1344.

[15] M. T. Sananes, A. Tuel, *Solid State Nucl. Mag.* **1996**, *6*, 157-166.

[16] a) J. Hietala, A. Vuori, P. Johnsson, I. Pollari, W. Reutemann, H. Kieczka in *Ullmann's Encyclopedia of Industrial Chemistry,* Wiley-VCH, Weinheim, **2016**, pp. 1-22, doi: 10.1002/14356007.a12_013.pub3; b) J. J. A. Celaje, Z. Lu, E. A. Kedzie, N. J. Terrile, J. N. Lo, T. J. Williams, *Nat. Commun.* **2016**, *7*, 11308-11313; c) D. Mellmann, P. Sponholz, H. Junge, M. Beller, *Chem. Soc. Rev.* **2016**, *45*, 3954-3988.

[17] C. Ratnasamy, J. P. Wagner, *Catal. Rev.*- Sci. Eng. **2009**, *51*, 325-440.

[18] J. Richard, R. Nielsen in *Handbook of Heterogeneous Catalysis, Ch. 13.11* (Eds.: G. .Ertl, H. Knözinger, F. Schüth, J. Weitkamp), Wiley-VCH, Weinheim, **2008**, pp. 2882-2905.

[19] J. D. Holladay, J. Hu, D. L. King, Y. Wang, *Catal. Today* **2009**, *139*, 244-260.

Entry for the Table of Contents

COMMUNICATION

Natural value: Highly selective CO production from methane over vanadium pyrophosphate *via* oxychlorination chemistry offers an exciting potential to exploit the stranded natural gas for the on-site manufacture of value-added chemicals and fuels.

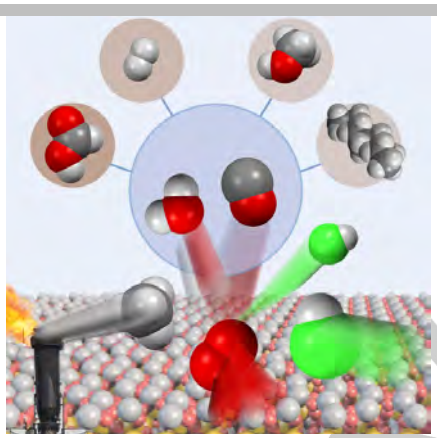

*Vladimir Paunović, Guido Zichittella, Réne Verel, Amol P. Amrute, Javier Pérez-Ramírez**

Page No. – Page No.
Selective Production of Carbon Monoxide *via* Methane Oxychlorination over Vanadyl Pyrophosphate

Angewandte Chemie
Eine Zeitschrift der Gesellschaft Deutscher Chemiker

Supporting Information

Selective Production of Carbon Monoxide via Methane Oxychlorination over Vanadyl Pyrophosphate

*Vladimir Paunović[+], Guido Zichittella[+], Réne Verel, Amol P. Amrute, and Javier Pérez-Ramírez**

anie_201608165_sm_miscellaneous_information.pdf

Methods

Catalyst preparation

Commercial CeO_2 (Sigma-Aldrich, nanopowder, 99.9%) was treated at 1173 K, while TiO_2 (Sigma-Aldrich, rutile nanopowder, 99.5%) and Nb_2O_5 (Sigma-Aldrich, 99.99%) were treated at 873 K for 5 h in static air prior to their use in the catalytic tests. RuO_2 was obtained by calcination in static air of anhydrous $RuCl_3$ (ABCR, 99.9%) at 823 K for 5 h. $LaVO_4$ was synthesized by dissolving $La(NO_3)_3 \cdot 6H_2O$ (10.83 g, Sigma-Aldrich, ≥99.6%) into freshly prepared 1 M HNO_3 (100 cm^3, Fisher Chemical, 65%) followed by gradual addition of NH_4VO_4 (Sigma-Aldrich, ≥99.5%) solution (2.92 g in 100 cm^3 of 1 M HNO_3). After adjusting the pH to 7 by dropwise addition of 2 M NaOH, the resulting solution was stirred for 4 h at room temperature and then transferred into a Teflon-lined autoclave. The hydrothermal synthesis was performed under autogenic pressure at 453 K for 24 h. The precipitate was separated by filtration, washed with deionized water, dried under vacuum (50 mbar) at 373 K for 6 h, and calcined at 873 K in static air. Vanadyl pyrophosphate (VPO) was prepared by refluxing a suspension of V_2O_5 (15 g, Aldrich, ≥99.6%) in isobutanol (90 cm^3, Acros, >99%) and benzyl alcohol (60 cm^3, Sigma Aldrich, >99%) for 3 h. After cooling down to room temperature, H_3PO_4 (Sigma Aldrich, ≥85%) was added to set the molar P:V ratio to 1.2 and the mixture was then refluxed for another 16 h. The resulting solid was recovered by filtration, washed with isobutanol and methanol (Fluka, ≥99.9%), dried in vacuum (50 mbar) at 373 K for 16 h, and thermally treated at 873 K under flowing N_2 (Pan Gas, purity 4.5) for 5 h. The thermal treatments of all catalysts were conducted using a heating rate of 5 K min^{-1}.

Catalyst characterization

Powder X-ray diffraction (XRD) was measured using a PANalytical X'Pert PRO-MPD diffractometer by applying Cu-Kα radiation. The data was recorded in the 10-70° 2θ range with an angular step size of 0.017° and a counting time of 0.26 s per step. N_2 sorption at 77 K was performed using a Quantachrome Quadrasorb-SI analyzer. Prior to the measurement, the sample was evacuated to 50 mbar at 573 K for 12 h. The Brunauer-Emmett-Teller (BET) method (Brunauer *et al.*, *J. Am. Chem. Soc.* **1938**, *60*, 309-319) was applied to calculate the total surface area, S_{BET}, in $m^2\ g^{-1}$. X-ray photoelectron spectroscopy (XPS) measurements were performed on a Physical Electronics Quantum 2000 X-ray photoelectron spectrometer using monochromatic Al-Kα radiation, generated from an electron beam operated at 15 kV, and equipped with a hemispherical capacitor electron-energy analyzer. The powdered sample were analyzed at the electron take-off angle of 45° and the pass energy of 46.95 eV. A compensation for sample charging was obtained by referencing all the spectra to the C 1*s* at 284.5 eV. Temperature-programmed reduction with H_2 (H_2-TPR) was conducted in Micromeritics Autochem II 2920 unit equipped with a thermal conductivity detector and coupled to a MKS Cirrus 2 mass spectrometer. The powder sample (0.05 g) was loaded in a U-shaped quartz reactor between two plugs of quartz wool, pretreated in He (20 cm^3 STP min^{-1}) at 623 K for 30 minutes, and cooled down to 500 K in He. H_2-TPR was then performed using 5 vol.% H_2 in N_2 (20 cm^3 STP min^{-1}) in a temperature range 500-1100 K with a ramp rate of 10 K min^{-1}. The ^{31}P nuclear magnetic spectra were acquired using the spin-echo mapping (Li *et al.*, *Appl. Catal.* **1991**, *73*,

83-95) or Variable Offset Cumulative Spectrum (VOCS) (Massiot *et al*., *Solid State Nucl. Mag.* **1995***, 4,* 241-248) method on a Bruker Avance IIIHD spectrometer equipped with a 9.4T Magnet (162.2 MHz ^{31}P Larmor frequency). Samples were loaded into 3.2mm rotors and measured using a 3.2mm Double Resonance MAS probe in *static* mode. For each sample, 7 experiments with a variation of the carrier frequency from 0 to 6000 ppm in 1000 ppm steps were combined. For each offset of the carrier frequency the tuning and matching of the probe was checked and adjusted. The individual experiments used a $\pi/2$-τ-π-acquire spin-echo sequence with a 16 step phase cycle. The $\pi/2$ pulse was set to 1.0 μs and the delay τ to 20 μs. A total of 512 scans were acquired with a recycle delay of 0.2 s. The possibility of saturation was tested by repeating a number of experiments with a recycle delay of 2.0 s. No difference between experiments with 0.2 s or 2.0 s recycle delay was observed. The full-echo time domain signals were processed and combined to a final skyline type spectrum using custom written Matlab scripts incorporating functions of the MatNMR toolbox (van Beek, *J. Magn. Reson.* **2007**, *187*, 19-26).

Catalytic evaluation

All the catalytic tests were performed at 1 bar in a continuous-flow fixed-bed reactor set-up (Scheme S1). The quartz reactor (10 mm internal diameter) was loaded with the catalyst (W_{cat} = 1.0 g, particle size = 0.4-0.6 mm) well mixed with quartz particles (particle size = 0.2-0.3 mm) in order to ensure a constant bed volume (V_{bed} = 1.8 cm^3) and placed in a homemade electrical oven equipped with a K-type thermocouple fixed in a coaxial quartz thermowell whose tip reaches the center of the catalyst bed. The catalyst was heated in a He flow till the desired bed temperature (T = 423-875 K) and stabilized for 30 min under these conditions before the introduction of the reaction mixture. Appropriate amounts of gases: CH_4 (PanGas, purity 5.0), CO (Messer, 5 mol.% in He with purity 5.0), HCl (Air Liquide, purity 2.8, anhydrous), HBr (Air Liquide, purity 2.8, anhydrous), CH_3Cl (PanGas, purity 2.8), CH_3Br (PanGas, 5 mol.% in He with purity 5.0), O_2 (PanGas, purity 5.0), Ar (PanGas, purity 5.0; internal standard), and He (PanGas, purity 5.0; carrier gas) were fed using digital mass flow controllers (Bronkhorst) to achieve a desired feed composition at a total volumetric flow, F_T, of 100 cm^3 STP min^{-1} (space velocity, F_T/W_{cat} = 100 cm^3 STP min^{-1} g^{-1}). CH_2Cl_2 (Sigma-Aldrich, 99.5%) and CH_2Br_2 (ABCR, 99%) were vaporized in the carrier gas stream using a syringe pump (Nexus 6000, Chemyx) and a homebuilt vaporizer operated at 343 K, accommodating a quartz T-connector filled with glass beads. Compositions of the feed mixtures used in the catalytic tests performed in this study are summarized in Table S1.

Condensation of the reactants and products in downstream lining was prevented by heating it at 393 K. The effluent stream from the catalytic reactor was neutralized by passing it through an impinging bottle containing aqueous NaOH solution (1 M). Prior to the analysis of the reactor outlet, the reaction was stabilized under given conditions for at least 1 h. The content of carbon-containing compounds (CH_4, CH_3Cl, CH_2Cl_2, CO, and CO_2) and Ar was determined on-line using a gas chromatograph equipped with a GS-Carbon PLOT column coupled to a mass spectrometer (GC-MS, Agilent GC 6890, Agilent MSD 5973N). To quantify H_2, the product mixture was first passed through

Table S1. Reactions and feed compositions studied in this work.

Reaction	Inlet concentration / vol.%							
	CH_4	CH_3X[a]	CH_2X_2	CO	HX	O_2	Ar	He
CH_4 oxyhalogenation	6	0	0	0	6	3	4.5 (85)[b]	80.5 (0)[b]
CH_4 oxidation	6	0	0	0	0	3	4.5	86.5
CH_3X oxidation	0	1	0	0	0	3	4.5	91.5
CH_2X_2 oxidation	0	0	1	0	0 (6)[c]	3	4.5	91.5 (85.5)[c]
CO oxidation	0	0	0	1	0 (6)[c]	3	4.5	91.5 (85.5)[c]
HX oxidation	0	0	0	0	6	3	4.5	86.5

[a] X denotes Cl or Br.

[b] The values in brackets refer to the concentration of Ar and He used in the tests in which H_2 production was quantified.

[c] The values in brackets refer to the concentration of HCl and He applied in the tests where HCl was co-fed with the main reactants.

an impinging bottle containing 0.1 M NaOH solution to neutralize HCl, followed by the collection of remaining stream in a gas bag. The concentration of H_2 in the sampled gas was analyzed using gas chromatograph (SRI 8610C) equipped with HayeSep D and Molecular Sieve 13X packed columns, and TCD detector. The Cl_2 was quantified by an iodometric titration (Mettler Toledo G20 Compact Titrator) of triiodide, formed by purging a stream containing a molecular halogen through an aqueous KI solution (0.1 M), with 0.01 M sodium thiosulfate solution (Aldrich, 99.99%).The concentration of HCl was determined by passing the outlet gas stream through an absorption tray comprising 2 impinging bottles filled with H_2SO_4 solution (Merck, 0.05 M) to absorb HCl, while dissolution of Cl_2 is strongly suppressed in acidic media. The amount of absorbed HCl, n(HCl), was quantified by titration with a NaOH standard solution (Merck, c_{NaOH} = 0.05 M) using Eq. 1,

$$n(\mathrm{HCl}) = (\Delta V_1 + \Delta V_2) \cdot c_{\mathrm{NaOH}}, \mathrm{mol} \qquad \text{Eq. 1}$$

where ΔV_1 and ΔV_2 represent the difference in volumes of NaOH consumed for the titration of H_2SO_4 solution after and prior to passing the outlet gas stream in the first and the second impinging bottle, respectively. In all experiments, ΔV_2 was close to 0, suggesting that most of HCl was absorbed in the first bottle.

The conversion of reactant i, $X(i)$, (i refers to CH_4, CH_3Cl, CH_3Br, CH_2Cl_2, CH_2Br_2, CO, or HCl) was calculated using Eq. 2,

$$X(i) = \frac{n(i)^{\mathrm{inlet}} - n(i)^{\mathrm{outlet}}}{n(i)^{\mathrm{inlet}}} \cdot 100, \% \qquad \text{Eq. 2}$$

where $n(i)^{inlet}$ and $n(i)^{outlet}$ are the amounts of the compound *i* at the inlet and outlet of the reactor, respectively, expressed in moles. In case of HCl and HBr oxidation, conversion of hydrogen halide, *X*(HX), was determined according to Eq. 3,

$$X(\mathrm{HX}) = \frac{2 \cdot n(\mathrm{X_2})^{outlet}}{n(\mathrm{HX})^{inlet}} \cdot 100, \% \qquad \text{Eq. 3}$$

where $n(X_2)^{outlet}$ and $n(HX)^{inlet}$ denote the amount of halogen and HX at the reactor outlet and inlet, respectively, expressed in moles. The selectivity to product *j*, *S*(*j*), (*j* refers to CH_3Cl, CH_2Cl_2, CO, or CO_2) was calculated based on Eq. 4,

$$S(j) = \frac{n(j)^{outlet} \cdot N_C(j)}{\sum^{outlet} n(j)^{outlet} \cdot N_C(j)} \cdot 100, \% \qquad \text{Eq. 4}$$

where $N_C(j)$ corresponds to the number of the carbon atoms in compound *j*. The selectivity to H_2, $S(H_2)$, was determined using Eq. 5,

$$S(\mathrm{H_2}) = \frac{2 \cdot n(\mathrm{H_2})^{outlet}}{n(\mathrm{CH_4})^{inlet} - n(\mathrm{CH_4})^{outlet}} \cdot 100, \% \qquad \text{Eq. 5}$$

where $n(H_2)^{outlet}$ denotes the amount of H_2 at reactor outlet, while $n(CH_4)^{inlet}$ and $n(CH_4)^{outlet}$ denote the amount of methane at reactor inlet and outlet, respectively. The yield of product *j*, *Y*(*j*), was calculated according to Eq. 6,

$$Y(j) = \frac{X(i) \cdot S(j)}{100}, \% \qquad \text{Eq. 6}$$

The error of the carbon balance, ε_C, was determined using Eq. 7,

$$\varepsilon_C = \frac{\sum^{inlet} n(i)^{inlet} \cdot N_C(i) - \left(n(\mathrm{CH_4})^{outlet} + \sum^{outlet} n(j)^{outlet} \cdot N_C(j) \right)}{\sum^{inlet} n(i)^{inlet} \cdot N_C(i)} \cdot 100, \% \qquad \text{Eq. 7}$$

The error of the chlorine balance, ε_{Cl}, in the oxychlorination experiments was calculated using Eq. 8,

$$\varepsilon_{\mathrm{Cl}} = \frac{n(\mathrm{HCl})^{inlet} - (n(\mathrm{HCl})^{outlet} + n(\mathrm{CH_3Cl})^{outlet} + 2 \cdot n(\mathrm{Cl_2})^{outlet} + 2 \cdot n(\mathrm{CH_2Cl_2})^{outlet})}{n(\mathrm{HCl})^{inlet}} \cdot 100, \% \qquad \text{Eq. 8}$$

The errors of the mass balances were lower than 5%. Each catalytic data point reported was determined as an average of at least two measurements. After the tests, the catalyst bed was quenched to room temperature in He flow. The catalyst was separated by sieving from the quartz particles and collected for *ex situ* characterization.

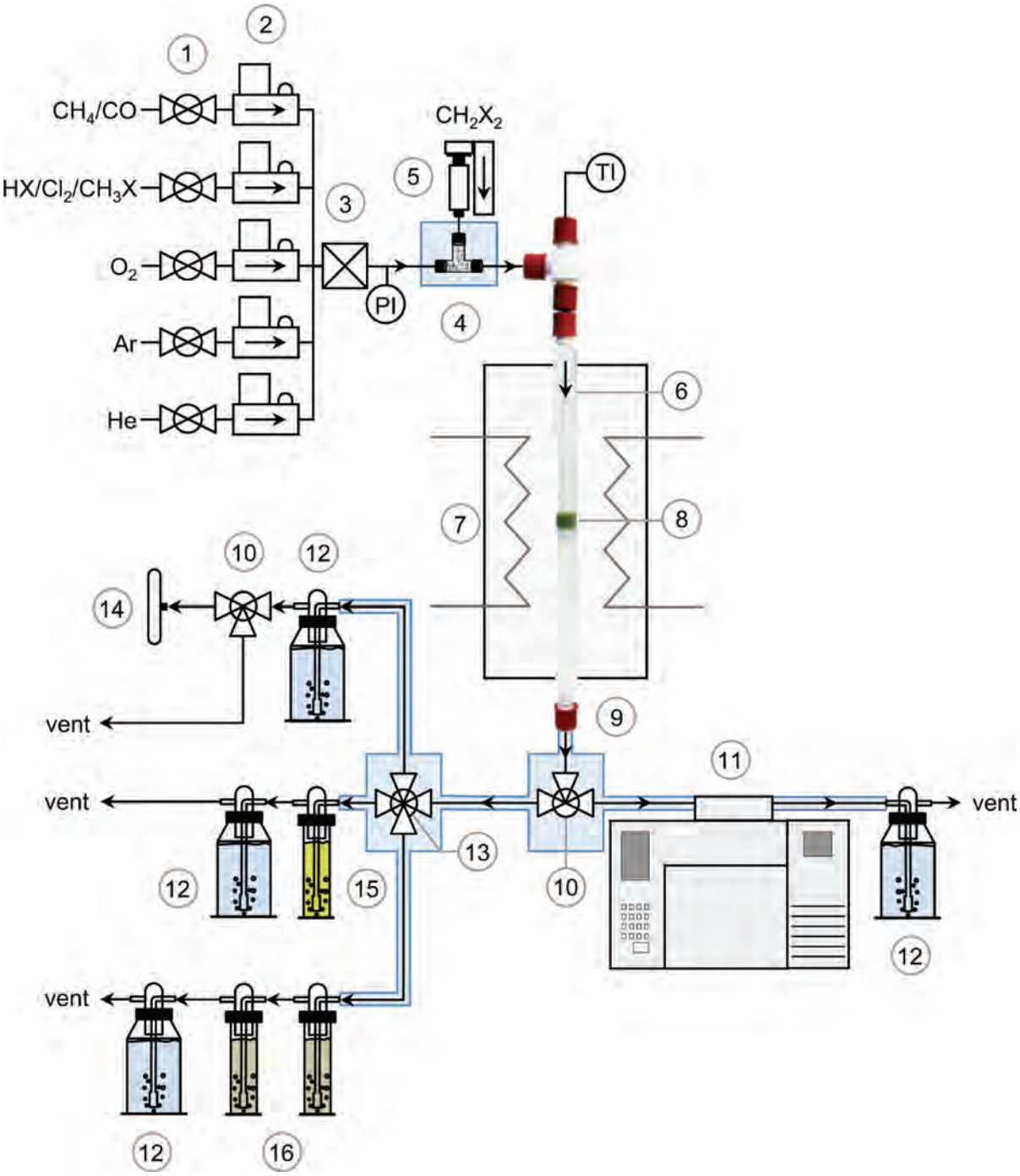

Scheme S1. Scheme of the laboratory set-up for the catalytic tests. 1: two-way on-off valves, 2: mass flow controllers, 3: mixer, 4: vaporizer, 5: syringe pump, 6: quartz reactor, 7: oven, 8: catalyst bed, 9: heat tracing, 10: three-way sampling valve, 11: GC-MS, 12: NaOH scrubber, 14: gas-sampling bag, 15: KI impinging bottle, 16: H_2SO_4 impinging bottles, PI: pressure indicator, and TI: temperature indicator.

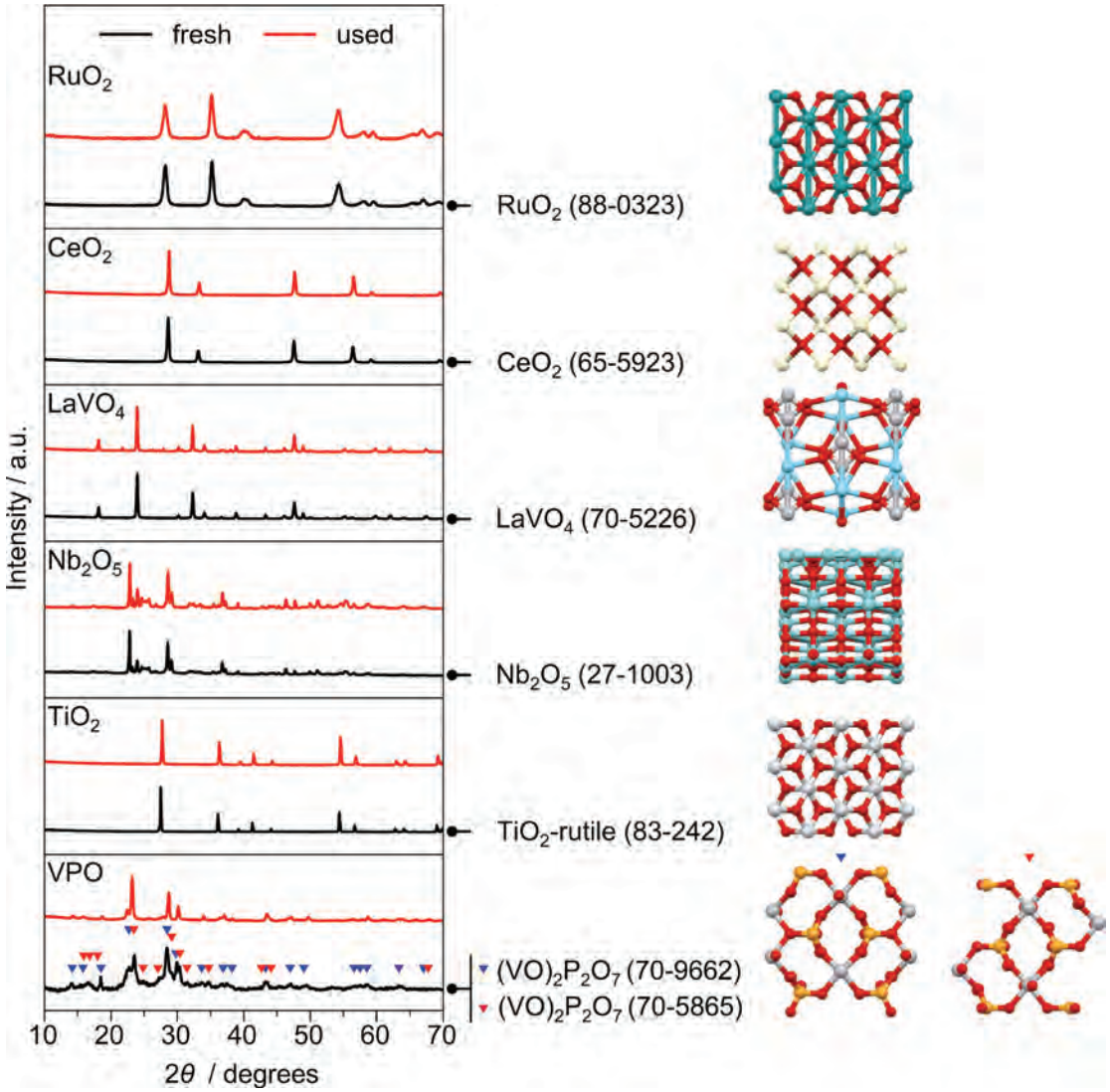

Figure S1. X-ray diffraction patterns of the samples prior to (fresh) and after (used) the oxychlorination of methane. The right panel denotes the identified crystalline phases and ICDD-PDF numbers.

Table S2. Total surface area of the catalysts, S_{BET}, prior to (fresh) and after (used) the oxychlorination of methane.

Catalyst	S_{BET} / m^2 g^{-1}	
	fresh	used
RuO_2	9	9
CeO_2	34	16
$LaVO_4$	15	5
Nb_2O_5	3	2
TiO_2	3	3
VPO	20	10

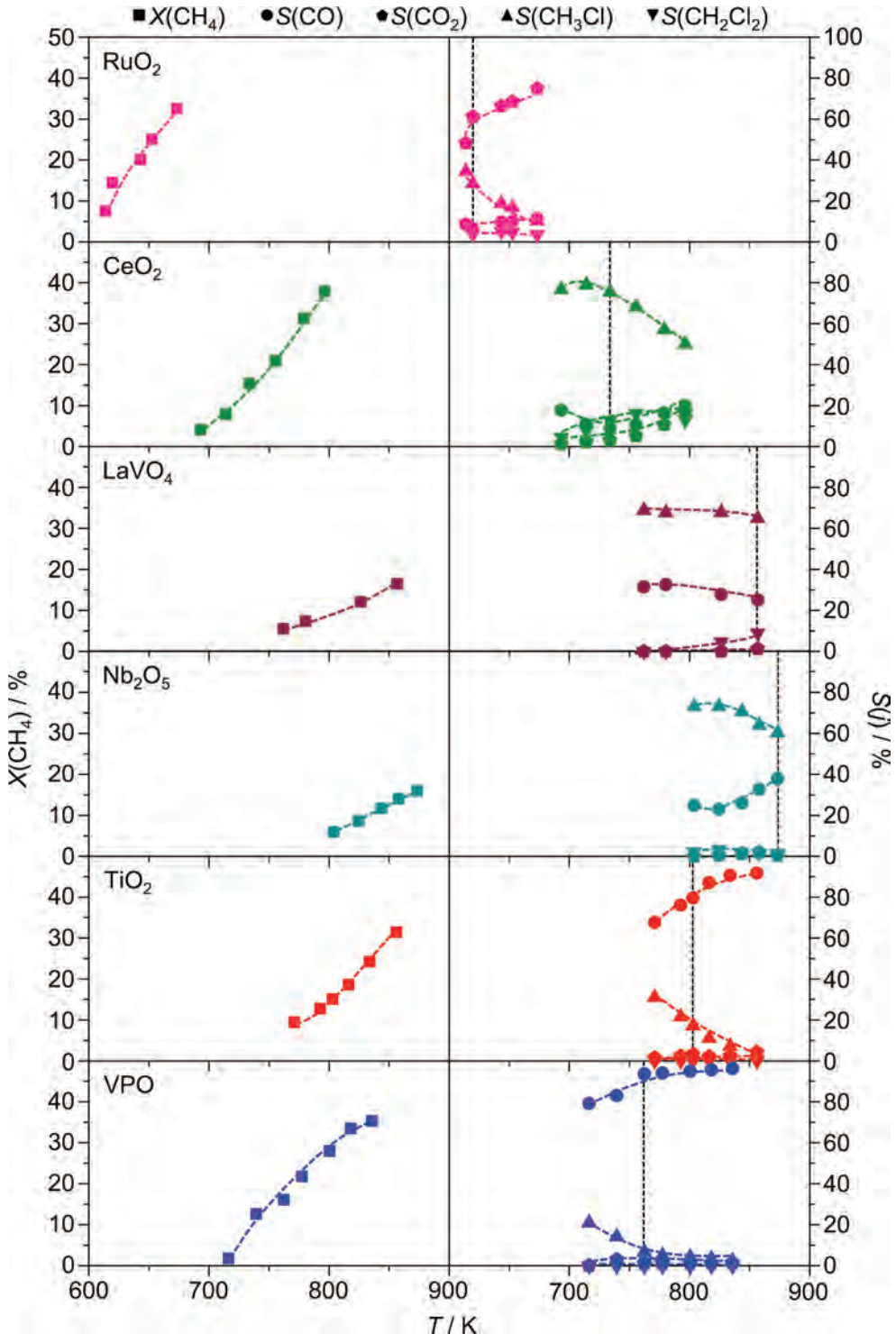

Figure S2. CH_4 conversion (left panel) and selectivity to product *j* (right panel) *versus* temperature in the oxychlorination of methane over different catalysts. Points lying on the vertical dashed lines correspond to product selectivities observed at *ca.* 15% methane conversion, which are presented in Figure 2 of the main manuscript. Conditions: F_T/W_{cat} = 100 cm^3 min^{-1} g^{-1}, CH_4:HCl:O_2:Ar:He = 6:6:3:4.5:80.5, and *P* = 1 bar.

Table S3. HCl conversion and selectivity to Cl_2 and H_2 in methane oxychlorination over VPO at different temperatures.

T / K	X(HCl) / %	$S(Cl_2)$ / %	$S(H_2)$ / %
762	1.5	16	0.05
777	1.3	<6	0.04
800	1.4	<6	0.04
818	1.2	<6	0.05
836	1.2	<6	0.06

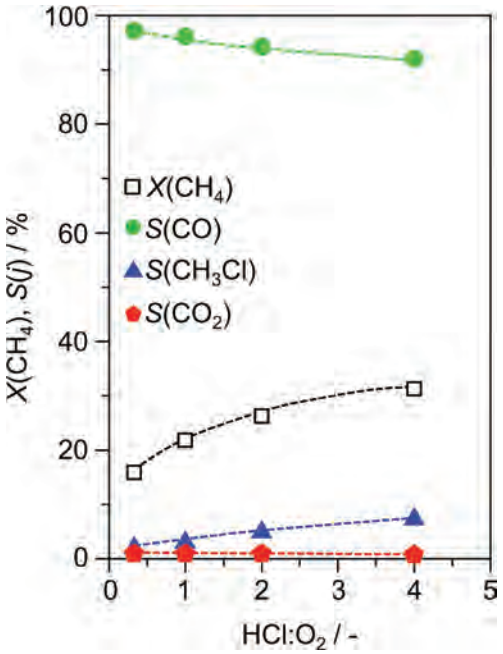

Figure S3. CH_4 conversion and product selectivity *versus* feed $HCl:O_2$ ratio in the oxychlorination of methane over VPO. Operation at high $HCl:O_2$ ratios favors the conversion of methane and slightly decreases the selectivity to CO. Conditions: F_T/W_{cat} = 100 cm^3 min^{-1} g^{-1}, CH_4:HCl:O_2:Ar:He = 6:1-12:3:4.5:85.5-74.5, T = 803 K and P = 1 bar.

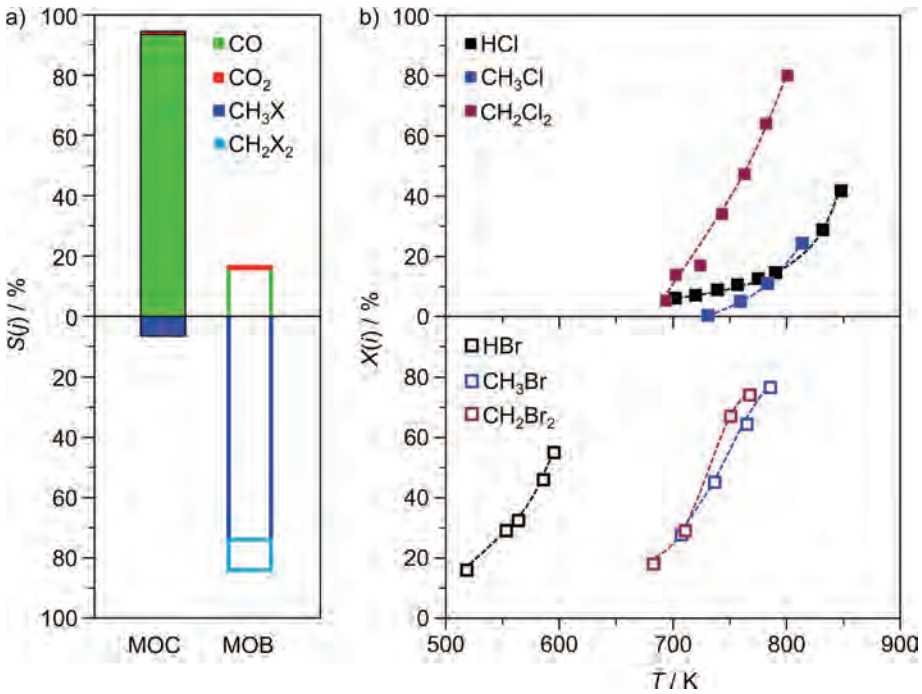

Figure S4. a) Product selectivity in methane oxychlorination (MOC, solid bars) and oxybromination (MOB, open bars) over VPO at *ca.* 15% methane conversion. A switch from MOC to MOB leads to a diametric change in product distribution, demonstrating the rich but complex nature of the oxyhalogenation chemistry. b) Conversion of HX, CH_3X, and CH_2X_2 *versus* temperature over VPO in the corresponding oxidation reactions. In case of X = Cl, the relative order of the light-off curves of HCl, CH_3Cl, and CH_2Cl_2 oxidation indicates that the rate of chloromethane oxidation is comparable (CH_3Cl) or higher (CH_2Cl_2) than the rate of HCl oxidation. The oxidation of HCl evolves molecular chlorine, Cl_2, which can react with methane to yield chloromethanes (especially di- and polychlorinated methanes, *i.e.*, CH_2Cl_2, $CHCl_3$, CCl_4) *via* gas-phase chlorination readily proceeding at $T \geq 673$ K (Olah *et al.*, *Beyond Oil and Gas: The Methanol Economy*, Wiley-VCH, **2009**, 233-278). In such a mechanism, the chlorine evolution through the heterogeneous HCl oxidation is likely to be the limiting step for chloromethane formation over VPO. Based on the proposed consecutive mechanism, comprising chloromethanes production followed by their oxidation over the same catalyst, a high selectivity to CO in the oxychlorination of methane might be explained by the fact that the rates of chloromethane oxidation are approximately equal or even higher (particularly in case of di- and polychlorinated methanes) compared to rates of their formation, resulting thus in a fast consumption of these intermediates once they are formed. In case of X = Br, the temperature for HBr oxidation is shifted by *ca.* 150 K to lower values compared to that where oxidation of CH_3Br and CH_2Br_2 occurs. On the other hand, gas-phase bromination, exhibiting inherently high selectivity to CH_3Br, onsets at >700 K (Paunović *et al.*, *Nat. Chem.* **2016**, *8*, 803-809), where most of the HBr is already converted into bromine. Following the same consecutive mechanism, a high selectivity to bromomethanes in the congeneric methane oxybromination might be rationalized by a significantly higher rate of HBr oxidation compared to that of bromomethanes, which preserves a high concentration of these intermediate compounds. Conditions: Methane oxyhalogenation: CH_4:HX:O_2:Ar:He = 6:6:3:4.5:80.5, HX oxidation: HX:O_2:Ar:He = 6:3:4.5:86.5, CH_3X oxidation: CH_3X:O_2:Ar:He = 1:3:4.5:91.5, CH_2X_2 oxidation: CH_2X_2:O_2:Ar:He = 1:3:4.5:91.5, F_T/W_{cat} = 100 cm^3 min^{-1} g^{-1}, and P = 1 bar.

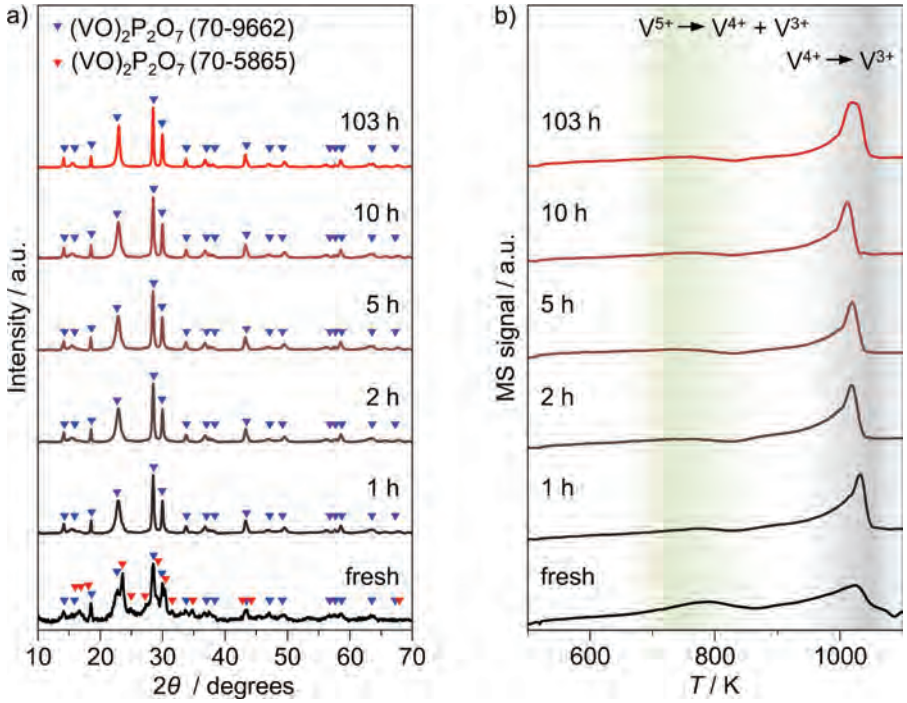

Figure S5. a) XRD patterns and b) H_2-TPR profiles of VPO prior to (fresh) and after the oxychlorination of methane for different time-on-stream (*x* h) at 803 K. The diffractogram of the fresh sample indicates that it is mainly composed of two $(VO)_2P_2O_7$ phases, in line with the P:V ratio of 1 as found by XRF analysis (Table S4). Exposure of the catalyst to the reaction mixture leads to its reconstruction into the originally present dominant $(VO)_2P_2O_7$ phase within the first hour. The latter phase is preserved during a 103 h on stream. H_2-TPR profiles of fresh and used samples demonstrate V^{4+} to be the dominant oxidation state of V, although a small contribution from V^{5+} reduction can be observed, in line with XPS data (Table S4, Figure S6). H_2-TPR profiles of used catalysts are essentially identical, while fresh catalyst shows a slightly broader peak in the region of V^{4+} reduction, and a bit more pronounced V^{5+} reduction peak.

Table S4. Characterization data of VPO samples prior to (fresh) and after (*x* h) the oxychlorination of methane for different time-on-stream (*x* h) at 803 K.

Sample	S_{BET} / $m^2\,g^{-1}$	P:V[a] / -	V oxidation state[b] / -	V^{5+}[c] / %
fresh	20	1.01	4.08	28
1 h	23	1.00	4.12	37
2 h	23	1.02	4.08	36
5 h	23	1.01	4.15	39
10 h	23	1.01	4.07	34
103 h	16	1.01	4.14	36

[a] Determined by XRF.

[b] Calculated based on O 1*s* and V 2*p* (3/2) core level binding energies (Figure S6), *BE*, using formula (Coulston *et al.*, *J. Catal.* **1996**, *163*, 122-129): V oxidation state = 13.82 – 0.68(Binding Energy(O 1*s*) – Binding Energy (V 2*p* (3/2))).

[c] Calculated based on deconvolution of V 2*p* (3/2) peak as shown in Figure S6.

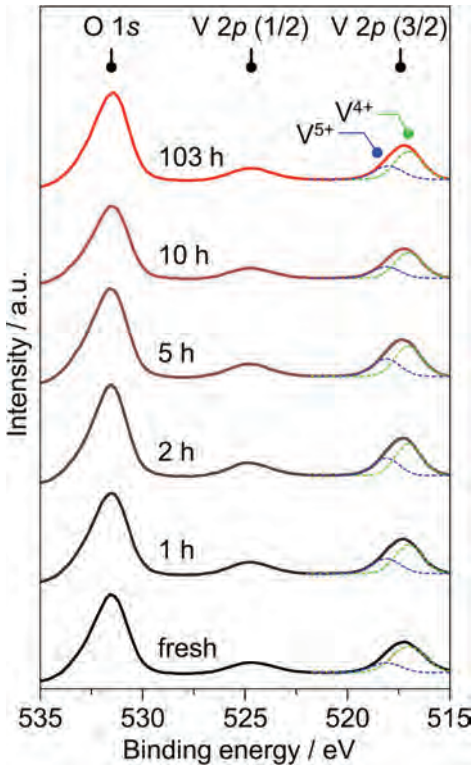

Figure S6. XPS spectra of VPO samples prior to (fresh) and after (*x* h) the oxychlorination of methane for different time-on-stream (*x* h) at 803 K. The binding energies of O 1*s* (*ca.* 532 eV) and V 2*p* (3/2) (*ca.* 517 eV) showed no significant deviations between the samples and are in good agreement with previous studies on VPO catalysts (Abon *et al*., *J. Catal.* **1995**, *156*, 28-36). A deconvolution of V 2*p* (3/2) peak into two peaks centered around 517.0 eV and 518.1 eV, which correspond to V^{4+} (literature values: 516.9-517.1 eV) and V^{5+} (literature values: 518.0-518.2 eV) states, respectively, showed the fraction of V^{5+} to be 28-39 % (Table S4). These differences in V^{5+} content fall in range of the error of the method (*ca.* 10%).